JOURNAL OF SOLID STATE CHEMISTRY 41, 213–220 (1982)

Heat Capacity of Iron–Chromium Spinels, $Fe_{3-x}Cr_xO_4$

HIDEAKI INABA, SETSUO NAKASHIMA, AND KEIJI NAITO

Department of Nuclear Engineering, Faculty of Engineering, Nagoya University, Furo-cho, Chikusa-ku, Nagoya, Japan

Received July 7, 1981; in final form September 2, 1981

The heat capacity of $Fe_{3-x}Cr_xO_4$ with the composition $x = 0.6$, 0.8, and 1.0 was measured from 200 to 850 K. A λ-type heat capacity anomaly due to the ferri–paramagnetic transition was observed for all compositions. The transition temperatures were 652, 563, and 451 K for the compositions $x = 0.6$, 0.8, and 1.0, respectively. The variation of transition temperature with composition is discussed in terms of cation distribution.The magnetic contribution to the observed heat capacity was obtained by assuming that the heat capacity is expressed by the sum of the lattice heat capacity C_v(l), the dilation contribution d(d), and the magnetic contribution C(m).Entropy changes due to the transition were calculated from C(m) as 52.6, 49.7, and 46.3 J K^{-1} $mole^{-1}$ for the compositions $x = 0.6$, 0.8, and 1.0, respectively, which are from 7 to 12 J K^{-1} $mole^{-1}$ higher than the calculated values based on the assumption of randomization of unpaired spins on each ion. The difference between the observed and the calculated values is roughly explained by taking into account the orbital contribution of Fe^{2+} ions on octahedral and tetrahedral sites.

1. Introduction

Iron–chromium spinels, $Fe_{3-x}Cr_xO_4$ ($0 \leq x \leq 2$), have the spinel structure, in which the metal ions partially occupy the tetrahedral (A site) and octahedral (B site) interstices of the close-packed oxygen lattice. Magnetite, $Fe^{3+}[Fe^{2+}Fe^{3+}]O_4$ ($x = 0$ in $Fe_{3-x}Cr_xO_4$), is an inverse spinel; $FeCr_2O_4$ ($x = 2$ in $Fe_{3-x}Cr_xO_4$) is a normal spinel; and $Fe_{3-x}Cr_xO_4$ with intermediate x have various cation distributions with different degrees of inversion. Various physical properties such as lattice constant (*1–4*), magnetic moment (*2, 3, 5*) and Mössbauer spectra (*5, 6*) have been measured as a function of composition x, and discussed in terms of the cation distribution among these sites.

In the mixed oxides such as $Fe_{3-x}Cr_xO_4$, the change in heat capacity due to the compositional change is usually small, as the Kopp–Neumann law predicts, as long as the classical lattice vibration is the predominant contribution to the heat capacity (*7, 8*). However, when a phase transition occurs, as in the case of TiO_x (*9*), $Ni_{1-x}Se_x$ (*10*), U_4O_{9-y} (*11*), and $Fe_{1-x}Co_xS_2$ (*12*), the heat capacity and resulting enthalpy and entropy changes due to the phase transition depend on composition, which should provide useful information on the mechanism of the phase transition.

In the previous study, heat capacities of $Mn_xFe_{3-x}O_4$ (*13*) with various x values were measured and the entropy change due to the transition as a function of x was interpreted as the sum of the contribution due to the randomization of unpaired electron spins and that due to the cation exchange reaction between the tetrahedral and the octahedral sites in the spinel structure.

Since $Fe_{3-x}Cr_xO_4$ exhibits a ferri–paramagnetic transition, it is expected that the

0022-4596/82/020213-08$02.00/0

heat capacity anomaly due to the transition should depend strongly on the composition x.

The heat capacities of $Fe_{3-x}Cr_xO_4$ have been measured for the end members; Fe_3O_4 ($x = 0$) by Gronvøld and Sveen (*14*), and $FeCr_2O_4$ by Naylor (*15*). Each study, however, was restricted to one composition, and no discussion on the composition dependence of the heat capacity has been reported.

2. Experimental

2.1. Sample Preparation

Samples of $Fe_{3-x}Cr_xO_4$ with the composition $x = 0.6$, 0.8, and 1.0 were prepared as follows: Fe_2O_3 and Cr_2O_3 of 99.99% purity were mixed in an appropriate metal composition and prefired for 4 hr at 800°C and then sintered for 12 hr at 1000°C in air. After that, the samples in a platinum basket were kept in an argon gas stream for about 5 hr at 1250°C using a high-frequency furnace, and then they were quenched to room temperature. The oxygen partial pressure due to the impurity oxygen included in the argon gas stream was kept to be around 10^{-5} atm, which was monitored by measuring the electrical conductivity of a nonstoichiometric cobalt oxide sensor (*16*) placed in the rear stream of the high-frequency furnace. The X-ray diffraction patterns of the sample powders showed cubic spinel phase. The observed lattice constants were 8.386 ± 0.003 Å for $x = 0.6$, 8.388 ± 0.003 Å for $x = 0.8$, and 8.399 ± 0.003 Å for $x = 1.0$.

2.2 Heat Capacity Measurement

Heat capacity of $Fe_{3-x}Cr_xO_4$ was measured by an adiabatic scanning calorimeter (*17*), where the power supplied to the sample was measured continuously, and the heating rate was maintained constant regardless of the kind and amount of sample. The heating rate chosen was 2 K min^{-1}, and the measurement was carried out between 200 and 850 K under nitrogen gas at about 2 Torr. The variations in the heating rate and in the adiabatic condition were maintained within ± 0.01 K min^{-1} and ± 0.02 K, respectively. The $Fe_{3-x}Cr_xO_4$ sample powder was sealed in a quartz glass vessel filled with helium gas at about 200 Torr. The sample amount used for the measurement was 7.3168 g for $Fe_{2.4}Cr_{0.6}O_4$, 6.4071 g for $Fe_{2.2}Cr_{0.8}O_4$, and 7.1321 g for Fe_2CrO_4.

3. Results and Discussion

3.1. Heat Capacity and Curie Temperature

The results of the heat capacity measurement on $Fe_{3-x}Cr_xO_4$ for the compositions $x = 0.6$, 0.8, and 1.0 are listed in Table I and are shown in Fig. 1. The imprecision of the heat capacity measurement of the present study was within $\pm 1\%$. As seen in Fig. 1, the λ-type heat capacity anomaly due to the ferri–paramagnetic transition becomes small and broad as x in $Fe_{3-x}Cr_xO_4$ increases. The difference in heat capacities due to different composition is small except for the temperature range of the transition, as the Kopp–Neumann law predicts.

In the dynamic calorimeter, a temperature difference is produced in the sample and a so-called scanning error is produced, as discussed in previous papers (*11, 17*). The scanning error was corrected by shifting the sample temperature by about 3 K in this study according to the method described earlier (*11, 17*). In order to determine the exact peak temperature of the heat capacity anomaly, the heat capacity around the peak temperature was measured at various heating rates, and excess heat capacities for various heating rates were calculated by subtracting the contributions due to the lattice vibration and the dilation using the method described later. Then the

TABLE I

HEAT CAPACITY OF $Fe_{3-x}Cr_xO_4$

	C_v(J K^{-1} mole^{-1})		
T (K)	(x = 0.6) $Fe_{2.4}Cr_{0.6}O_4$ (MW = 229.23)	(x = 0.8) $Fe_{2.2}Cr_{0.8}O_4$ (MW = 228.46)	(x = 1.0) Fe_2CrO_4 (MW = 227.69)
200	116.6	116.9	115.2
220	125.1	126.7	126.5
240	135.1	135.1	135.3
260	142.3	144.6	144.4
280	149.9	152.3	152.3
300	157.2	160.7	160.9
320	162.1	166.0	165.8
340	166.9	171.7	171.7
360	171.8	176.2	177.4
380	176.6	181.0	182.8
400	181.7	185.1	188.3
420	186.6	189.4	192.2
440	191.8	194.4	196.4
460	198.0	200.5	198.5
480	203.5	205.1	199.2
500	209.3	209.8	200.2
520	215.0	214.0	200.4
540	219.4	217.7	199.9
560	225.5	220.1	199.6
580	229.5	219.2	198.6
600	233.8	213.3	198.0
620	239.3	210.8	197.6
640	242.8	207.7	197.0
660	244.5	204.5	196.0
680	225.9	202.0	196.5
700	218.2	200.4	195.9
720	213.0	199.6	195.3
740	208.9	198.5	194.6
760	204.9	197.5	194.7
780	203.9	197.4	195.1
800	201.9	197.4	195.2
820	200.9	—	—
840	198.7	—	—

peak temperatures were obtained at various heating rates, from which the transition temperature was determined by extrapolating the heating rate to zero. The Curie temperature thus determined is plotted against composition in Fig. 2, where the previous results by Francombe (*2*) and Robbins et al. (*5*) determined by magnetic measurement are also shown for comparison. The results by Francombe and Robbins *et al.* differ from each other by up to 40 K between the compositions $x = 0$ and 1.0, probably due to systematic error of the measurements or different methods of sample preparation; the results of the present work lie between the two previous works. As seen in Fig. 2, the plot of Curie temperature against composition deviates significantly from a linear dependence; it slowly decreases in the region $0 \leq x \leq 0.7$ and $1.3 \leq x \leq 2.0$, whereas it sharply decreases in the region $0.7 \leq x \leq 1.3$. This dependence is quite different from the case of $Fe^{3-x}Mn_xO_4$, where the Curie temperature decreases linearly with the manganese content x in the region $1.0 \leq x \leq 2.0$ (*13*). These different behaviors may be understood in terms of cation distribution as follows (*5*).

The cation distribution of $Fe_{3-x}Cr_xO_4$ has been measured by means of Mössbauer spectrocopy (*5*) and X-ray diffraction (1.2) and is summarized by the formula (*18*):

$$Fe^{3+}_{1-y}Fe^{2+}_y[Fe^{2+}_{1-y}Fe^{3+}_{1-x+y}Cr^{3+}_x]O_4, \quad (1)$$

$$y = 0.3x, \qquad 0 \leq x \leq 0.3, \quad (1a)$$

$$y = 0.6(x - 0.2), \qquad 0.3 \leq x \leq 0.7, \quad (1b)$$

$$y = x - 0.4, \qquad 0.7 \leq x \leq 1.3, \quad (1c)$$

$$y = \tfrac{1}{7}(x + 5), \qquad 1.4 \leq x \leq 2.0, \quad (1d)$$

where the symbols ahead of the brackets denote cations in tetrahedral (A) sites, and those inside the brackets denote cations in octahedral (B) sites; y denotes the degree of inversion. Similarly, the cation distribution

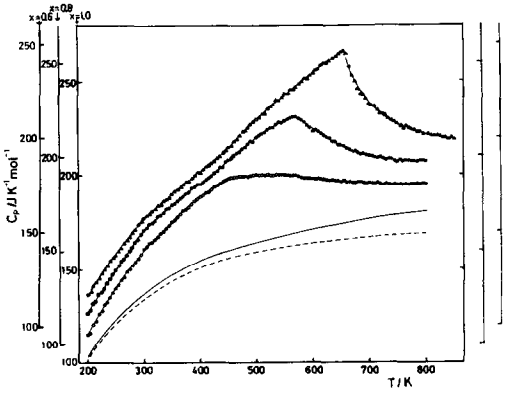

FIG. 1. Heat capacity of $Fe_{3-x}Cr_xO_4$: (7) x = 0.6, (●) x = 0.8, (○) x = 1.0. Vertical axis is shifted to upper side by 10 and 20 J K^{-1} mole^{-1} for x = 0.8 and x = 0.6, respectively. (——) C_v(I) + C_d, x = 1.0, ---- C_v(I), x = 1.0.

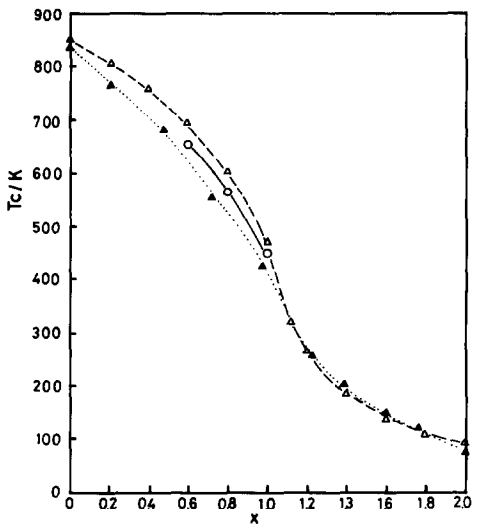

FIG. 2. Curie temperature of $Fe_{3-x}Cr_xO_4$ against chromium content: (○) this work, (△) Francombe, (▲) Robbins *et al.*

of $Mn_xFe_{3-x}O_4$ is given by the formula (*19*):

$$Mn^{2+}_{1-y}Fe^{3+}_{y}[Mn^{2+}_{y}Mn^{3+}_{x-1}Fe^{3+}_{3-y-x}]O_4, \quad 1.0 \le x \le 2.0. \quad (2)$$

In the case of $Mn_xFe_{3-x}O_4$, the degree of inversion y increases linearly with x (*20*) to give a linear change of the cation distribution with x, which is thought to result in the linear decrease of the Curie temperature with x. On the other hand, in the case of $Fe_{3-x}Cr_xO_4$, the cation distribution given in Eq. (1) shows that the slopes of the four linear equations (1a–d) representing the x–y relationship change, depending on the composition range x; it is 0.3 for $0 \le x \le 0.3$, 0.6 for $0.3 \le x \le 0.7$, 1.0 for $0.7 \le x \le 1.3$ and ½ for $1.4 \le x \le 2.0$. This tendency corresponds to the slope of the decreasing curve of Curie temperature with x in Fig. 2; it is low for $0.0 \le x \le 0.3$, higher for $0.3 \le x \le 0.7$, highest for $0.7 \le x \le 1.3$, and lowest for $1.4 \le x \le 2.0$. In the range $0.7 \le x \le 1.3$, for example, the increase of Cr^{3+} content results in the decrease of the same amount of Fe^{3+} in the A site according to Eq. (1c). This decreases the strength of the Fe^{3+}–Fe^{3+} (A–B) interaction and decreases the Curie temperature sharply, because the Fe^{3+}–Fe^{3+} (A–B) interaction is responsible for the high Curie temperature of inverse ferrite spinels such as $NiFe_2O_4$.

3.2. Resolution of the Heat Capacity and the Entropy Change Due to the Transition

The observed heat capacity of $Fe_{3-x}Cr_xO_4$ is considered to be a sum:

$$C_p = C_v(l) + C(d) + C(m), \quad (3)$$

where $C_v(l)$ is the lattice heat capacity at constant volume, $C(d)$ the dilation contribution, and $C(m)$ the magnetic contribution.

(1) Lattice heat capacity at constant volume. We have no available data to calculate this main contribution of the compound $Fe_{3-x}Cr_xO_4$ with intermediate x. However, it would be reasonable to assume that $Fe_{3-x}Cr_xO_4$ is a solid solution between the two end members $x = 0$ and $x = 2$: Fe_3O_4 and $FeCr_2O_4$; in such a case, the Debye temperature of $Fe_{3-x}Cr_xO_4$ can be obtained by interpolation between $x = 0$ and $x = 2$. The Debye temperature of Fe_3O_4 has been determined as 605 K (*10*) from the heat capacity data at low temperatures by averaging the value of Debye temperature over the region 180 to 200 K after subtracting the spin-wave contribution (*21*). No value for the Debye temperature of $FeCr_2O_4$ has been reported, but the lattice heat capacity of $FeCr_2O_4$ can be estimated by using the same method applied to $MgAl_2O_4$ (*22*), $CoFe_2O_4$ (*23*), and $NiFe_2O_4$ (*23*) by Grimes and to $Mn_xFe_{3-x}O_4$ (*13*) by the present authors as shown below.

The lattice heat capacity is expressed as a linear combination of Debye and Einstein functions and each characteristic phonon frequency is determined from the four fundamental infrared absorption bands ν_1, ν_2, ν_3, and ν_4, as follows (*24*),

$$C_v(1) = 2E(\theta_1/T) + 2D(\theta_2/T) + 2E(\theta_3/T) + D(\theta_4/T), \quad (4)$$

$$\theta_n = hc/k\,\nu_n = 1.438\,\nu_n, \quad (5)$$

where E and D are Einstein and Debye functions, respectively, θ_n the characteristic temperature, h Planck's constant, k Boltzmann's constant, c the light velocity, and ν_n the infrared absorption frequency in inverse centimeters. The infrared spectrum of $FeCr_2O_4$ has been reported; ν_1 and ν_2 are 617 and 523 cm^{-1}, respectively, as cited by Vatolin *et al.* (*25*), and ν_3 and ν_4 are 377 and 177 cm^{-1}, respectively, as cited by Shiratori (*26*). Using these data and Eqs. (4) and (5), $C_v(l)$ for $FeCr_2O_4$ may be determined. In order to obtain a single Debye characteristic temperature for $FeCr_2O_4$, $C_v(l)$ thus obtained is fitted to a single Debye function at 200 K and the resulting single Debye temperature is determined to be 785 K. By using the Debye temperatures of Fe_3O_4 and $FeCr_2O_4$, the individual Debye temperatures of $Fe_{3-x}Cr_xO_4$ at 200 K can be interpolated to be 659 K for $Fe_{2.4}Cr_{0.6}O_4$, 677 K for $Fe_{2.2}Cr_{0.8}O_4$, and 695 K for Fe_2CrO_4, $C_v(l)$ for each sample is obtained by using a single Debye function. For Fe_2CrO_4 it is shown in Fig. 1 as a broken line, for example.

(*2*) *The dilation contribution.* The dilation contribution at constant pressure, $C(d)$, is evaluated as follows:

$$C(d) = Cp - C_v = \alpha^2 VT/\kappa \quad (6)$$

$$\simeq \alpha\Gamma C_v T, \quad (7)$$

where α is the expansivity, V the molar volume, κ the compressibility, and Γ is the Grüneisen constant which is expressed as $\Gamma = \alpha V/\kappa C_v$ and does not strongly depend on temperature. However, since neither the expansivity nor the compressibility of $Fe_{3-x}Cr_xO_4$ with composition $x = 0.6$, 0.8, and 1.0 has been reported (in the temperature range of the present study), the Grüneisen constant Γ and the expansivity α of $Fe_{3-x}Cr_xO_4$ with $x = 0.6$, 0.8, and 1.0 are assumed to be equal to those of Fe_3O_4, in order to calculate $C(d)$ of Eq. (7). The expansivity of Fe_3O_4 was reported by Gorton *et al.* (*26*) and the Grüneisen constant for Fe_3O_4 was determined as 1.75 by Grønvold and Sveen (*10*). Thus $C(d)$ for $Fe_{3-x}Cr_xO_4$ is calculated and $C_v(l) + C(d)$ for Fe_2CrO_4 is shown in Fig. 1 in a solid line.

(*3*) *The magnetic contribution.* The magnetic contribution $C(m)$ is obtained by subtracting $C_v(l)$ and $C(d)$ from the observed heat capacity C_p according to Eq. (3). $C(m)$ obtained for $Fe_{3-x}Cr_xO_4$ is shown in Fig. 3, showing usual λ-type curves. In Fig. 3, solid lines below 200 K represent the magnetic heat capacity calculated by using Grimes (*23*) equation. The Grimes equation for magnetic heat capacity is based on the spin-wave theory for the ferrites discussed by Kaplan (*28*), and Glasser and Milford (*29*), and expressed as follows,

$$C(m) = F_1 + F_2 + E(12\,J_{AB}S_A/kT) + \tfrac{1}{3}E(24\,J_{AB}S_B/kT), \quad (8)$$

where F_1 and F_2 are the contributions of heat capacity due to an acoustic and an optical branch of the spin wave, respectively. The last two terms represent the

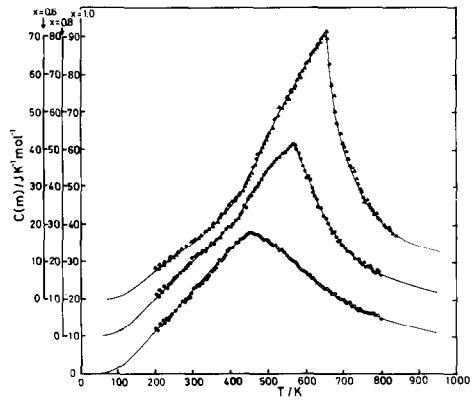

FIG. 3. Magnetic heat capacity of $Fe_{3-x}Cr_xO_4$ (△) $x = 0.6$, (●) $x = 0.8$, (○) $x = 1.0$. Vertical axis is shifted to upper side by 10 and 20 J K^{-1} mole $\frac{1}{8}^{-1}$ for $x = 0.8$ and $x = 0.6$, respectively.

Einstein function due to optical branches of the spin wave, J_{AB} is the exchange interaction energy between A and B sites, and S_A and S_B are the average spin values at each site. In a reasonable approximation, F_1 is reduced to the following equation:

$$F_1 = 0.113R(kT/Z)^{3/2} \quad (9)$$

where R is the gas constant, k is the Boltzmann constant and $z = 11J_{AB}S_AS_B/2(2S_B - S_A)$. F_1 is the main contribution of the magnetic heat capacity, and the other three terms in Eq. (8) can be neglected near 0 K, but they become important as temperature increases. Grimes (*23*) showed that the excess heat capacities of $CoFe_2O_4$ and $NiFe_2O_4$ were in good agreement with the magnetic heat capacities calculated from Eq. (8) up to 300 K. In the case of $MnFe_2O_4$ (*13*), it was shown by the authors that J_{AB} determined by fitting Eq. (8) to the magnetic heat capacity between 200 and 250 K was in good agreement with that obtained by means of inelastic neutron scattering (*30*). The magnetic heat capacity of $Fe_{3-x}Cr_xO_4$ can be calculated from Eq. (8) by determining the three parameters: J_{AB}, S_A, and S_B. S_A and S_B were determined by assuming that the cation distribution of $Fe_{3-x}Cr_xO_4$ can be expressed by Eq. (1), and J_{AB} was determined by fitting the data of C(m) to Eq. (8) between 200 and 250 K. C(m) below 200 K was then calculated. The calculated parameters are assembled in Table II. Although we have no available data on J_{AB} to compare with those obtained by other methods, the calculated values 2.43, 2.24, and 2.22 meV for $Fe_{2.4}Cr_{0.6}O_4$, $Fe_{2.2}Cr_{0.8}O_4$, and $FeCr_2O_4$, respectively, are considered to be reasonable when compared to the values 2.4 meV for Fe_3O_4 as determined by neutron inelastic scattering (*31, 32*), and to 2.28 and 2.84 meV for $CoFe_2O_4$ and $NiFe_2O_4$, respectively, as obtained from the magnetic heat capacity (*23*). However, in order to obtain accurate J_{AB} values, the contributions of J_{AA} and J_{BB}, which are neglected in Eq. (8) and become important as Cr^{3+} content in $Fe_{3-x}Cr_xO_4$ increases, must be taken into account (*5*).

TABLE II

EXCHANGE INTERACTION ENERGY BETWEEN A AND B SITES AND AVERAGE SPIN VALUES S_A AND S_B AS A FUNCTION OF x IN $Fe_{3-x}Cr_xO_4$

x	J_{AB} meV	S_A	S_B
0.6	2.43	2.38	2.01
0.8	2.24	2.30	1.95
1.0	2.22	2.20	1.90

Since the heat capacity measurement in the present study was carried out up to 850 K for $Fe_{2.4}Cr_{0.6}O_4$ and to 800 K for $Fe_{2.2}Cr_{0.8}O_4$ and Fe_2CrO_4, the magnetic heat capacity C(m) above these temperatures was estimated by extrapolation, assuming that the magnetic heat capacity obeys the relationship $C(m)T^2 = \text{const.}$ (*33*) sufficiently far above the transition temperature. The extrapolation is shown as broken lines in Fig. 3. From Fig. 3, the entropy change due to the transition ΔS_m(exp.) was calculated by integrating $C(m)/T$ up to very high temperatures. The results are 52.6 ± 4.8, 49.7 ± 4.5, and 46.3 ± 4.4 J K^{-1} $mole^{-1}$ for the compositions $x = 0.6$, 0.8, and 1.0, respectively; they are plotted against composition in Fig. 4. For the end member of $Fe_{3-x}Cr_xO_4$, i.e., Fe_3O_4, Grønvold and Sveen (*10*) have obtained ΔS_m(exp.) using the same analysis and calculated a value of 55.3 J K^{-1} $mole^{-1}$, which is also shown in Fig. 4.

The origin of the ferri–paramagnetic transition is thought to be the randomization of unpaired electron spins of each ion; then the entropy change due to the transition can be calculated, assuming that the cation distribution is expressed by Eq. (1), as follows:

$$\Delta S_{spin} = R[\ln 5 + (2 - x)\ln 6 + x \ln 4], \quad 0 \le x \le 2, \quad (10)$$

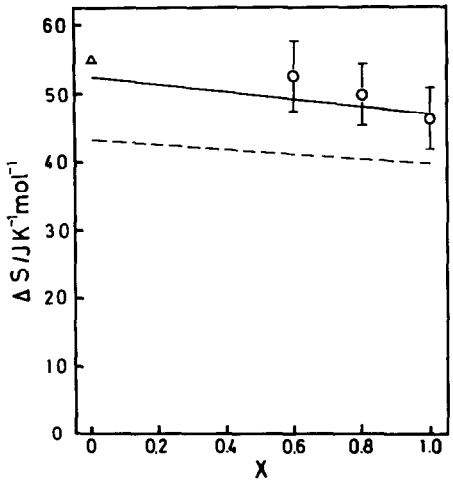

FIG. 4. Entropy change due to transition as a function of x in $Fe_{3-x}Cr_xO_4$.

where R is the gas constant. It is noted from Eq. (10) that ΔS_{spin} is independent of the degree of inversion y. ΔS_{spin} is shown against composition as a broken line in Fig. 4. As seen in the figure, the experimental values are 7 to 12 J K^{-1} $mole^{-1}$ higher than the calculated ones. This difference suggests that there is another contribution to the heat capacity.

Grønvold and Sveen (*10*) explained the difference between the experimental and the theoretical entropy changes for Fe_3O_4 by taking into account the orbital contribution to heat capacity due to Fe^{2+} ion in octahedral site to give an additional entropy change R ln 3 or 9.1 J K^{-1} $mole^{-1}$. This is a reasonable hypothesis given that in other octahedral Fe^{2+} compounds, for example, FeF_2, the ground T_{2g} level is split into three levels; the two higher levels are 1100 and 1300 K above the ground level as determined by Mössbauer study (*34*). As for $Fe_{3-x}Cr_xO_4$, this kind of orbital contribution to the heat capacity should be taken into account, since there are octahedral Fe^{2+} ions. As seen in Eq. (1), tetrahedral Fe^{2+} also exists in $Fe_{3-x}Cr_xO_4$, depending on the degree of inversion y. In the tetrahedral case, the E_g ground level is split into two levels; the energy difference between the upper orbital state and the ground state of tetrahedral Fe^{2+} of R_2FeCl_4 has been measured by Elward *et al.* (*35*) and Gibb and Greenwood (*36*), ranging from 266 to 690 K, depending on the organic component R. The additional entropy of this term is calculated to be R ln 2 or 5.8 J K^{-1} $mole^{-1}$. Since $Fe^{3+}(3d^5)$ and octahedral $Cr^{3+}(3d^3)$ have a nondegenerate ground state, the orbital contribution of these ions is regarded as negligibly small. The total additional entropy change by the orbital contributions is calculated using the cation distribution expressed in Eq. (1) as follows,

$$\Delta S_{orb} = (1 - 0.3x)R \ln 3 + 0.3xR \ln 2, \quad 0 \le x \le 0.3, \quad (11a)$$

$$\Delta S_{orb} = (1.2 - 0.6x)R \ln 3 + (0.6x - 0.12)R \ln 2, \quad 0.3 \le x \le 0.7, \quad (11b)$$

$$\Delta S_{orb} = (1.4 - x)R \ln 3 + (x - 0.4)R \ln 2, \quad 0.7 \le x \le 1.3, \quad (11c)$$

where x is the chromium content in $Fe_{3-x}Cr_xO_4$ and R is the gas constant. $(\Delta S_{spin} + \Delta S_{orb})$ are shown plotted against composition as a solid line in Fig. 4. The calculated $\Delta S_{spin} + \Delta S_{orb}$ are in agreement with the observed values ΔS_m(exp) within experimental error. It should be noted here that the estimation of ΔS_m may include a considerable error due to the lack of the required input data to calculate $C_v(1) + C_d$.

The possibility of other contributions to the entropy change, such as the contribution by conduction electrons, and by cation exchange reactions between the tetrahedral and the octahedral sites, should be considered. Grønvold and Sveen (*10*) estimated the contribution due to the conduction electrons for Fe_3O_4 as C(c.e.) = 0.004 (T/K) J K^{-1} $mole^{-1}$, and the entropy change of this term was regarded as 2 J K^{-1} $mole^{-1}$. There is no way to estimate this term for

$Fe_{3-x}Cr_xO_4$, but this term must be less than 2 J K^{-1} $mole^{-1}$ and decreases as x increases, because the electronic conduction is mainly governed by electronic hopping between Fe^{2+} and Fe^{3+} at the octahedral sites. According to Navrotsky and Kleppa (*37*), the difference in the site preference energy between Mn^{2+} and Fe^{3+} is very small and the exchange reaction between the tetrahedral and octahedral sites has to be considered at higher temperatures in $Mn_xFe_{3-x}O_4$ (*13*). However, in the case of $Fe_{3-x}Cr_xO_4$, Cr^{3+} strongly prefers the octahedral site; the differences in the site preference energy between Cr^{3+} and Fe^{2+}, and between Cr^{3+} and Fe^{3+} are 20 and 27 kcal $mole^{-1}$, respectively. Thus the exchange reaction between the tetrahedral and the octahedral sites may not have to be taken into account.

References

1. H. J. YEARIAN, J. M. KORTRIGHT, AND R. H. LANGENHEIM, *J. Chem. Phys.* **22,** 1196 (1954).
2. M. H. FRANCOMBE, *J. Phys. Chem. Solids* **3,** 37 (1957).
3. W. D. DERBYSHIRE AND H. J. YEARIAN, *Phys. Rev.* **112,** 1603 (1958).
4. H. J. LEVINSTEIN, M. ROBBINS, AND C. CAPIO, *Mater. Res. Bull.* **7,** 27 (1972).
5. M. ROBBINS, G. K. WERTHEIM, R. C. SHERWOOD, AND D. N. E. BUCHANAN, *J. Phys. Chem. Solids* **32,** 717 (1971).
6. H. FRANKE AND M. ROSENBERG, *J. Magn. Magn. Mater.* **9,** 74 (1979).
7. H. INABA AND K. NAITO, *J. Solid State Chem* **15,** 283 (1975).
8. H. INABA AND K. NAITO, *Netsu* **4,** 10 (1977).
9. M. KOIWA AND H. HIRABAYASHI, *J. Phys. Soc. Japan* **27,** 801 (1969).
10. F. GRØNVOLD, N. J. KVESETH, AND A. SVEEN, *J. Chem. Thermodyn.* **7,** 716 (1975).
11. H. INABA AND K. NAITO, *J. Nucl. Mater.* **49,** 181 (1973).
12. S. OWAGA, *J. Phys. Soc. Japan* **41,** 462 (1976).
13. K. NAITO, H. INABA, AND H. YAGI, *J. Solid State Chem.* **36,** 28 (1981).
14. F. GRØNVOLD AND A. SVEEN, *J. Chem. Thermodyn.* **6,** 859 (1974).
15. B. F. NAYLOR, *Ind. Eng. Chem.* **36,** 933 (1944).
16. K. NAITO, N. KAMEGASHIRA, AND T. YUTANI, unpublished work.
17. K. NAITO, H. INABA, M. ISHIDA, Y. SAITO, AND H. ARIMA, *J. Phys. E* **7,** 464 (1974).
18. J. B. GOODENOUGH, *J. Phys. Chem. Solids* **25,** 151 (1964).
19. F. E. LOTGERING AND A. M. V. DIEPEN, *J. Phys. Chem. Solids* **34,** 1369 (1973).
20. G. D. RIECK AND F. C. M. DRIESSENS, *Acta Crystallogr.* **20,** 521 (1966).
21. E. F. WESTRUM AND F. GRØNVOLD, *J. Chem. Thermodyn.* **1,** 543 (1969).
22. N. W. GRIMES, *Spectrochim. Acta A* **28,** 2217 (1972).
23. N. W. GRIMES, *Proc. Roy. Soc. London Ser. A* **338,** 209 (1974).
24. R. D. WALDRON, *Phys. Rev.* **99,** 1727 (1955).
25. N. A. VATOLIN, A. V. SEREBRYAKOVA, P. I. VOLKOVA, S. V. SHIVAEVA, AND N. N. BELYAEVA, *Tr. Inst. Khim. Ural. Nauchn. Tsentr. Akad. Nauk SSSR* **35,** 119 (1976).
26. K. SHIRATORI, *J. Phys. Soc. Japan* **23,** 948 (1967).
27. A. T. GORTON, G. BITSIANES, AND T. L. JOSEPH, *Trans. Metall. Soc. AIME* **233,** 1519 (1965).
28. T. A. KAPLAN, *Phys. Rev.* **109,** 782 (1958).
29. M. L. GLASSER AND F. J. MILFORD, *Phys. Rev.* **130,** 1783 (1963).
30. W. WEGNER, D. SHEERLINCK, E. LEGRAND, S. HAUTECLER, AND V. A. M. BRABERS, *Solid State Commun.* **15,** 345 (1974).
31. H. WATANABE AND B. N. BROCKHOUSE, *Phys. Lett.* **1,** 189 (1962).
32. F. J. MILFORD AND M. L. GLASSER, *Phys. Lett.* **2,** 248 (1962).
33. J. S. SMART, "Effective Field Theories of Magnetism," Saunders, Philadelphia (1966).
34. U. GNIEL AND S. SHTRIKMAN, *Phys. Rev.* **177,** 503 (1969).
35. P. R. EDWARDS, C. E. JOHNSON, AND R. J. P. WILLIAMS, *J. Chem. Phys.* **47,** 2074 (1967).
36. T. C. GIBB AND N. N. GREENWOOD, *J. Chem. Soc.* 6989 (1965).
37. A. NAVROTSKY AND O. J. KLEPPA, *J. Inorg. Nucl. Chem.* **29,** 2701 (1967).